PEDS Advance Access published July 14, 2009

Protein Engineering, Design & Selection pp. 1–6, 2009
doi:10.1093/protein/gzp037

Short protein segments can drive a non-fibrillizing protein into the amyloid state

Poh K. Teng[1,2] and David Eisenberg[1,2,3]

[1]Departments of Biological Chemistry and [2]Chemistry and Biochemistry, UCLA-DOE Institute for Genomics and Proteomics, Howard Hughes Medical Institute, Molecular Biology Institute, UCLA, Box 951570, Los Angeles, CA 90095-1570, USA

[3]To whom correspondence should be addressed.
E-mail: david@mbi.ucla.edu

Protein fibrils termed amyloid-like are associated with numerous degenerative diseases as well as some normal cellular functions. Specific short segments of amyloid-forming proteins have been shown to form fibrils themselves. However, it has not been shown in general that these segments are capable of driving a protein from its native structure into the amyloid state. We applied the 3D profile method to identify fibril-forming segments within the amyloid-forming human proteins tau, alpha-synuclein, PrP prion and amyloid-beta. Ten segments, six to eight residues in length, were chosen and inserted into the C-terminal hinge loop of the highly constrained enzyme RNase A, and tested for fibril growth and Congo red birefringence. We find that all 10 unique inserts cause RNase A to form amyloid-like fibrils which display characteristic yellow to apple-green Congo red birefringence when observed with cross polarizers. These six to eight residue inserts can fibrillize RNase A and are sufficient for amyloid fibril spine formation.

Keywords: amyloid/domain swapping/functional networks/prion structure/protein interactions

Introduction

Amyloid fibrils are unbranched, fibrous aggregates associated with several degenerative diseases (Westermark *et al*., 2007), as well as denatured globular proteins (Astbury and Dickinson, 1935; Dobson, 1999), bacterial inclusion bodies (Wang *et al*., 2008) and several normal cellular functions (Si *et al*., 2003; Sekijima *et al*., 2005; Wang *et al*., 2008). Fibrils appear to arise from the spontaneous opening of proteins, the exposure of fibril-forcing segments and subsequent self-assembly. These fibrils share an enriched β-structure reflected in a cross-β diffraction pattern and Congo red birefringence (Glenner *et al*., 1972; Klunk *et al*., 1989; Sunde *et al*., 1997; Serpell *et al*., 2000). The atomic structures of GNNQQNY and NNQQNY of the *Saccharomyces cerevisiae* Sup35 prion revealed the atomic nature of the cross-β spine architecture: a steric zipper consisting of two interdigitating β-sheets (8.5 Å apart in this case) mating at a dry, complementary interface. Each sheet is built by stacking of identical segments along the fibril direction, separated by 4.9 Å (Nelson *et al*., 2005). Hydrogen bonds hold each sheet together, and van der Waals interactions bind the two sheets into the zipper spine.

The 3D profile method was used to identify segments within a protein that have high propensity to form a steric zipper by self-complementation, and hence possibly drive fibrillation of the protein (Thompson *et al*., 2006). In this method, every six-residue segment of a target protein is threaded onto the steric zipper template of NNQQNY. By optimizing the interdigitation, and using the RosettaDesign energy (Rohl *et al*., 2004), we calculated binding energies for putative steric zippers. Those with binding energies below an empirical threshold were predicted to form fibrils, and the results were validated by experiments (Ivanova *et al*., 2006; Thompson *et al*., 2006). Atomic structures of fibril-like microcrystals of these segments show a common cross-β spine architecture with subtle geometrical differences (Sawaya *et al*., 2007).

Ribonuclease A is an exceptionally stable and well-characterized enzyme (Libonati and Gotte, 2004; Smith and Raines, 2006; Marshall *et al*., 2008), cross-linked by four disulfide bonds, particularly suitable for experiments on induced fibrillation. In our experience of over 15 years of work with RNase A (Liu *et al*., 1998, 2001), the wild-type enzyme never forms amyloid-fibrils, even in a wide variety of destabilizing and denaturing solvents. Because the wild-type sequence does not form fibrils, we used RNase A to test the sufficiency of a polyglutamine insert for inducing amyloid fibril formation (Sambashivan *et al*., 2005). This work involved domain-swapped dimers. It was long known that RNase A is capable of forming domain-swapped oligomers (Crestfield *et al*., 1962). A C-terminal domain swapped dimer can form when a β-strand with residues 116–124 is exchanged between two subunits (Fig. 1) (Liu *et al*., 1998, 2001). The swapped domain is connected to the core domain (residues 1–111) by the hinge loop of residues 112–115. Hinge loops from both subunits undergo a conformational change to align in space so that they bridge both subunits of the dimer. The dimer is held together by interactions at the interface between the swapped domain and the core domain. The enzymatic activity of both functional units of RNase A is preserved. When a 10-residue polyglutamine segment was inserted in the hinge loop and the modified sequence was concentrated in mild acid, RNase A formed amyloid-like fibrils via domain-swapping (Sambashivan *et al*., 2005). An atomic model was built showing that it is possible to form an amyloid-like fibril, with domain-swapped RNase A molecules maintaining their native structure around a steric-zipper, cross-β spine.

The present study tests the ability of high propensity, fibril-forcing segments to drive fully cross-linked RNase A enzyme into the amyloid state. We show that segments of six to eight residues from human proteins tau, alpha-synuclein (α-syn), prion (PrP) and amyloid-beta (Aβ) are sufficient to induce RNase A into amyloid-like fibrils. Our observations support previous work that suggest short peptide segments are important structural components of the amyloid fibril core (Lansbury *et al*., 1995; von Bergen *et al*., 2000;

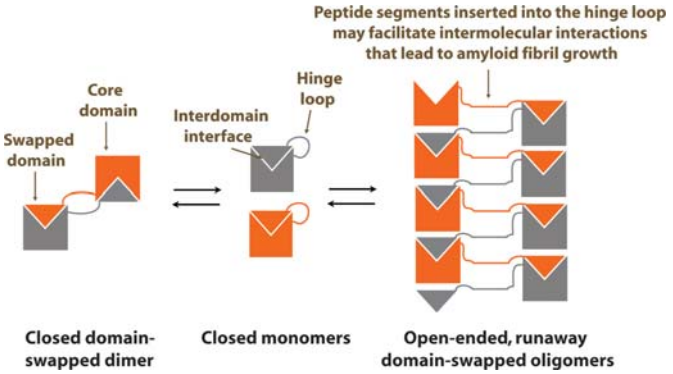

Fig. 1. The core domain of RNase A (residues 1–111) is connected to its C-terminal β-strand (residues 116–124) by a hinge loop (residues 112–115). Normal monomeric RNase A can be converted to domain-swapped dimers and higher order oligomers which retain native activity with composite active sites formed from segments of two molecules. We inserted fibril-forcing segments predicted to form steric zippers into the hinge loop between G112 and N113. RNase A constructs with these various insertions were tested for formation of amyloid fibrils, which may be the result of open-ended, runaway domain-swapping, as suggested by Sambashivan *et al.* (2005).

Balbirnie *et al*., 2001; von Bergen *et al*., 2001; Luhrs *et al*., 2005; Sawaya *et al*., 2007; Vilar *et al*., 2008).

Materials and methods

Fibril-forming segment prediction

Sequences of human proteins tau, α-syn, PrP and Aβ, and bovine pancreatic RNase A were analyzed with the 3D profiling method (Thompson *et al*., 2006) for fibril-forcing segments that form a steric zipper. With NNQQNY of the *S.cerevisiae* Sup35 as the backbone template, the binding energies of six to eight residue segments from these proteins were calculated. Fibril-forcing segments chosen for this study have energetic scores equal to, or less than, -3.7 kcal/mol/residue, which is the threshold for fibril formation via self-complementation (Thompson *et al*., 2006).

Design of constructs

Two inactive RNase A mutants in the pET-32b vector were previously engineered by site-directed mutagenesis to generate H12A and H119A variants (Sambashivan *et al*., 2005). These two mutants were provided as templates to GenScript Corporation for the insertion of selected human prion- and amyloid-related segments, between residues G112 and N113 of the RNase A C-terminal hinge loop region. The H119A variant was also used as template for the insertion of GSRSRT from tau by site-directed mutagenesis in the same location. All constructs were confirmed by DNA sequencing.

Protein expression and purification

Each new RNase A construct in pET-32b was transformed into BL21-CodonPlus(DE3)-RIPL cells (Agilent Technologies). Cells were grown in Teriffic Broth with 0.2% glucose, 0.4% glycerol and 100 μg/ml Ampicillin to an OD_{600nm} of 0.8–1.2. Protein expression was induced with 200 μM IPTG at 18°C for 20 h.

Cells were harvested by centrifugation at 6000*g* for 15 min. Cells were resuspended in 500 mM NaCl, 20 mM Tris pH 8.0 with protease inhibitors and lysed by sonication at 4°C. Cell debris was pelleted by centrifugation at 30 000*g* for 30 min, after which the supernatant was filtered with a 0.2-μm filter.

RNase A constructs were purified as described in Sambashivan *et al*. (2005), with the following changes. Pre-filtered supernatant for each construct was loaded onto a Hi-Trap Ni-NTA column (GE Healthcare) and eluted with an increasing imidazole gradient of 0–250 mM, in 500 mM NaCl, 20 mM Tris pH 8.0. Fractions with eluted protein were pooled and dialyzed against enterokinase buffer. Each sample was digested overnight with enterokinase (Invitrogen) and reloaded onto a Ni-NTA column. The flow-through containing cleaved RNase A protein was collected and dialyzed overnight against 100 mM NaCl.

Fibril formation

Purified RNase A constructs were concentrated to an apparent concentration of 5–12 mg/ml, as detected by protein absorbance at 280 nm with dilutions made in 6 M Gdn-HCl, 100 mM Tris pH 8. Samples were incubated in 50% (v/v) acetic acid for an hour at room temperature, and later, lyophilized. Freeze-dried samples were resuspended in water to an apparent final concentration of 35 mg/ml and stored at room temperature.

Electron microscopy

Samples were applied to hydrophilic 400-mesh, carbon-coated, formvar films mounted on copper grids (Ted Pella, Inc.). After 2.5 min, samples were rinsed twice with 0.2-μm filtered water and subsequently stained with 1–2.5% uranyl acetate. Samples were dried and examined with a Hitachi H-7000 transmission electron microscope (TEM) at 75 keV or with a Phillips CM120 TEM at 120 keV.

Congo red assay

The Congo red assay was carried out as described in Ivanova *et al*. (2006), with modifications. RNase A constructs that form fibrils were centrifuged at 20 000*g*. A pellet was observed in all samples post-centrifugation. Each pellet was washed twice by resuspension in 0.1-μm filtered water, centrifugation at 20 000*g* and removal of the supernatant. Each pellet was then resuspended in 100 μl of 0.1 mg/ml Congo red in 150 mM NaCl, 10 mM Tris pH 8.0 and incubated at room temperature for 30 min. After dye incubation, each sample was centrifuged for 5 min at 20 000*g*. The supernatant was discarded and the pellet was washed with 0.1-μm filtered water until the wash is no longer tainted red. Each pellet is resuspended in 5–20 μl of 0.1-μm filtered water. Sample drops were pipetted onto dust-free silanized coverslips and allowed to dry overnight in a dust-free petri dish. Dried samples were examined with an optical microscope in bright field and with cross polarizers.

Results

Fibril-forming segments predicted to form self-complementary steric zippers

Sequences for human tau, α-syn, PrP and Aβ were analyzed for fibril-forcing segments that form self-complementary steric zippers. Ten peptide segments from these proteins were chosen from a list of segments found to score equal to,

Table I. Fibril-forming segments inserted in the C-terminal hinge loop are from various human prion and amyloid proteins

Peptide segment	Protein	Rosetta binding energy per residue (kcal/mol)	Fibrils of RNase A+insert	Congo red birefringence
^{275}VQIINK^{280}	Tau	−4.2	Observed	+/−
^{306}VQIVYK^{311}	Tau	−4.3	Observed	++
^{50}GVATVA^{55}	α-syn	−4.5	Observed	+ +
^{65}NVGGAVVT^{72}	α-syn	−3.9	Observed	+
^{68}GAVVTG^{73}	α-syn	−4.4	Observed	+
^{74}VTAVAQKT^{81}	α-syn	−4.2	Observed	+
^{94}GTHSQW^{99}	PrP	−4.1	Observed	+/−
^{113}AGAAAA^{118}	PrP	−4.0	Observed	+
^{127}GYMLGS^{132}	PrP	−3.7	Observed	+
^{37}GGVVIA^{42}	Aβ	−4.6	Observed	++
^{149}GSRSRT^{154}	Tau	−2.0	Not observed	+/−
GGGGGGGGG[a]	n/a	−3.0	Not observed	n/a

The intensities of Congo red birefringence observed with cross polarizers are scored: ++, strong birefringence; +, birefringence; +/−, weak birefringence; −, no birefringence. Notice that the two negative control segments (below the double line) have predicted Rosetta binding energies above the threshold level, and do not force RNase A into fibril formation.
[a]Sambashivan *et al*., 2005.

or less than, −3.7 kcal/mol/residue (Table I). Two of these segments are eight residues long, while each of the remaining eight segments has six residues. All segments were also evaluated for area buried and shape complementarity at the predicted steric zipper interface (data not shown). These values were comparable to those calculated for NNQQNY of the *S.cerevisiae* Sup35 (Nelson *et al*., 2005).

Fibril-forming segments from prion and amyloid proteins induce RNase A to form fibrils

RNase A gains the ability to form fibrils when the predicted fibril-forming segments are inserted in its C-terminal hinge loop (between G112 and N113) (Fig. 2). Each inserted fibril-forming segment, shown in Table I, expands the hinge loop by six to eight residues, distancing 12 residues at the C-terminus of RNase A, shown in green in Fig. 2, from the rest of the molecule, shown in pink. Fibrils were formed by all 10 constructs in identical conditions, as described in the Materials and Methods section, but with varying incubation times. Wild-type RNase A and the inactive H119A RNase A that lacks a fibril-forming insertion do not form fibrils under the same condition (data not shown). RNase A with an insertion of GSRSRT from tau, predicted to be unfavorable in forming a steric zipper, does not form fibrils (Fig. 2; Table I). Similarly, RNase A with a nine-glycine insertion was previously found not to form fibrils (Sambashivan *et al*., 2005).

The RNase A fibrils are unbranched with widths in the range of 70–120 Å. However, they vary in persistence length, the tendency to form either aligned bundles or less-ordered tangles, and in their resemblance either to flat ribbons or twisted threads in a cord. Electron micrographs show fibril morphologies that are representative for each RNase A construct (Fig. 2).

Induced RNase A fibrils are in the amyloid state

RNase A fibrils induced by fibril-forcing segments share structural features with amyloid proteins; the fibrils display a yellow to apple-green birefringence when dyed with Congo red and examined between crossed polarizers (Fig. 3). This specific feature of amyloid (Glenner *et al*., 1972; Klunk *et al*., 1989) is exhibited by these RNase A fibrils with varying degrees of intensity (Table I). Inactive H119A RNase A without a fibril-forming insertion binds to Congo red, but lacks birefringence when observed with crossed polarizers (Fig. 3).

Discussion

Fibril-forming segments are fibril-forcing inserts

Our study focuses on 10 short (six to eight residues) protein segments, predicted by the 3D profile method to form steric zippers. Crystallographic structures have shown to date that 6 of these 10 segments do in fact form steric zippers (Sawaya *et al*., 2007). The atomic structures of the remaining four segments are as yet unknown. When each of these 10 segments is inserted into the C-terminal hinge loop of RNase A, the enzyme is converted to the amyloid state.

Three of these segments from α-syn have been found in previous work to be essential in forming a stable fibril core. In α-syn fibrils, NVGGAVVT (residues 65–72), GAVVTG (residues 68–73) and VTAVAQKT (residues 74–81) lie in β-strands 3 and 4 of a five-layered, β-sandwich fold (Vilar *et al*., 2008). Because deletion of these β-strands renders α-syn incapable of forming fibrils, they were proposed to be positioned in the fibril core (Vilar *et al*., 2008). In the present study, all three segments induce RNase A fibrils, the shorter GAVVTG subsegment of NVGGAVVT being sufficient to force RNase A into the amyloid state. In the β-sandwich model, GVATVA (residues 50–55) lies in β-strand 2, adjacent to β-strand 3 (Vilar *et al*., 2008), and we have shown that it too is sufficient to force RNase A fibril formation. In addition, an A53T mutation in the GVATVA segment was found to increase the aggregation propensity of α-syn, and lead to early onset of familial Parkinson's disease (Conway *et al*., 1998; El-Agnaf *et al*., 1998; Narhi *et al*., 1999; Li *et al*., 2001). It has not been determined if a GVTTVA segment is more capable than GVATVA in forming RNase A fibrils. It is not known whether GVTTVA enhances steric zipper formation or participates in long-range interactions that stabilize the overall β-structure of α-syn fibrils. In any case, Congo red birefringence observed in all the α-syn-RNase A constructs suggests that these tested segments can force β-sheet formation when inserted in the context of a globular protein. Neurotoxicity of α-syn is correlated with an increase in β-sheet structure from its native, random coil conformation (Serpell *et al*., 2000; Kim *et al*., 2007; Sandal *et al*., 2008). Although the β-sandwich model proposes that interactions between these segments hold the fibril core together (Vilar *et al*., 2008), our results show that each segment is sufficient for the formation of an amyloid fibril core by self-complementation.

Similarly, for Aβ in Alzheimer's disease, previous studies have shown that the segment GGVVIA (residues 37–42) is important in its pathogenesis. This segment was determined to form the fibril core of Aβ by mutagenesis and solid-state

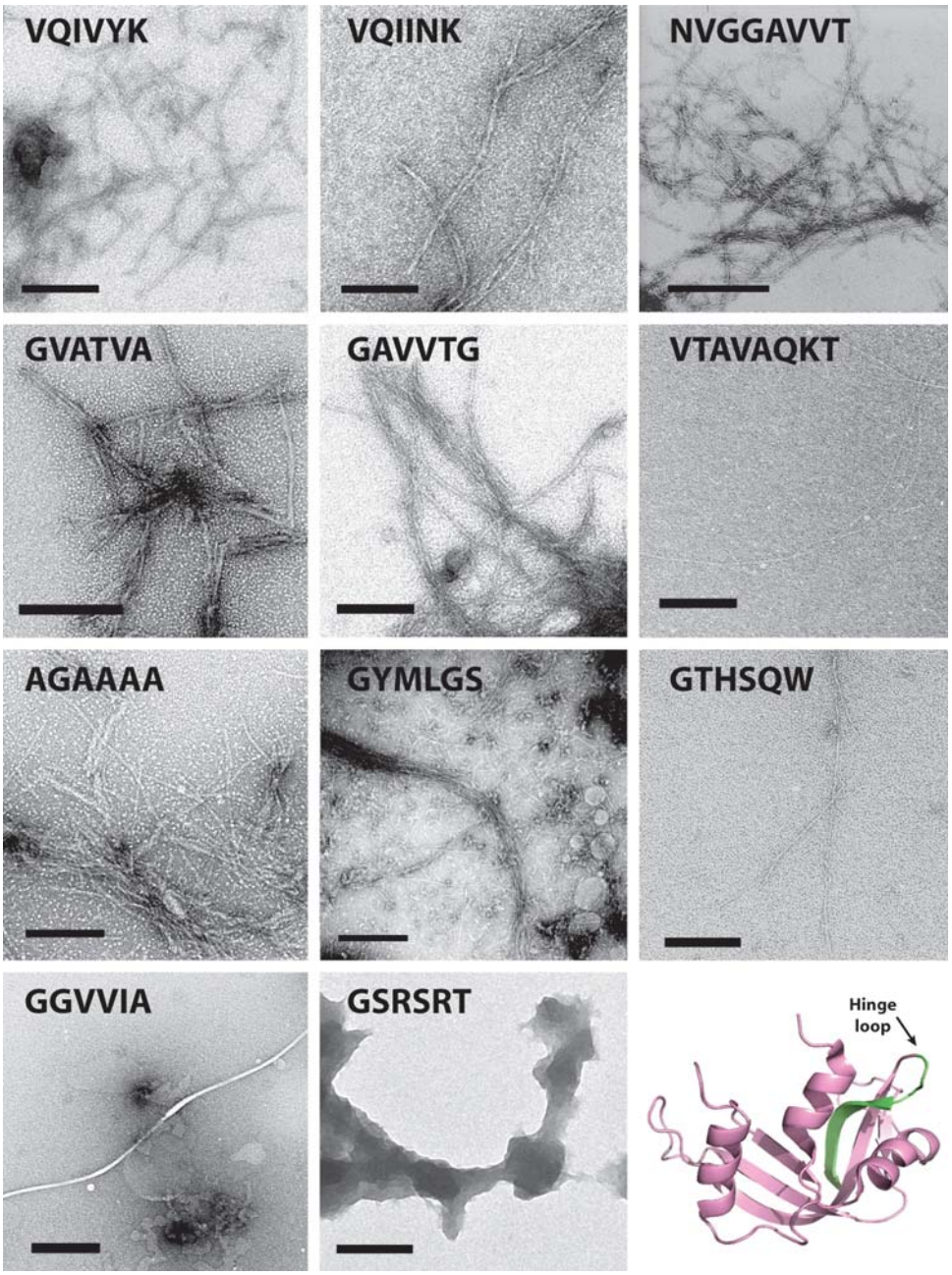

Fig. 2. Insertion of predicted fibril-forming segments induces the formation of RNase A fibrils. Each electron micrograph is labeled with the sequence of the insertion into the RNase A C-terminal hinge loop. All insertions are fibril-forming segments except GSRSRT, which is the only insert that does not cause fibrillation. Each insertion sits between the C-terminal β-strand, colored green, and the core domain of RNase A, shown in pink in the bottom-right panel of the figure. All scale bars are 200 nm.

nuclear magnetic resonance, while a G37D mutation in this segment decreases Aβ cell toxicity (Lansbury *et al*., 1995; Kanski *et al*., 2002; Luhrs *et al*., 2005). The power of this segment to drive fibrillation is emphasized by our observation that GGVVIA is sufficient to force RNase A to form amyloid fibrils.

Fibril-forming segments force RNase A into the amyloid state

All induced RNase A fibrils in this study are in the amyloid state, as shown by Congo red binding and birefringence. Inactive H119A RNase A that lacks a fibril-forming insertion binds to Congo red, but does not display birefringence. Negatively charged Congo red may bind to positively charged RNase A (pI = 9.3) via electrostatic interactions (Liu *et al*., 1998), or bind to β-sheets in the native structure of RNase A. The lack of birefringence when observed between cross polarizers presumably reflects the absence of a steric zipper spine.

Similarly, the non-fibril-forming segment GSRSRT when inserted into RNase A displays weak Congo red birefringence although no fibril formation was observed. The GSRSRT segment is predicted to be weak in forming a steric zipper spine. Insertion of GSRSRT may allow RNase A to open up its native structure, allowing RNase A to sample more conformations and form new intermolecular

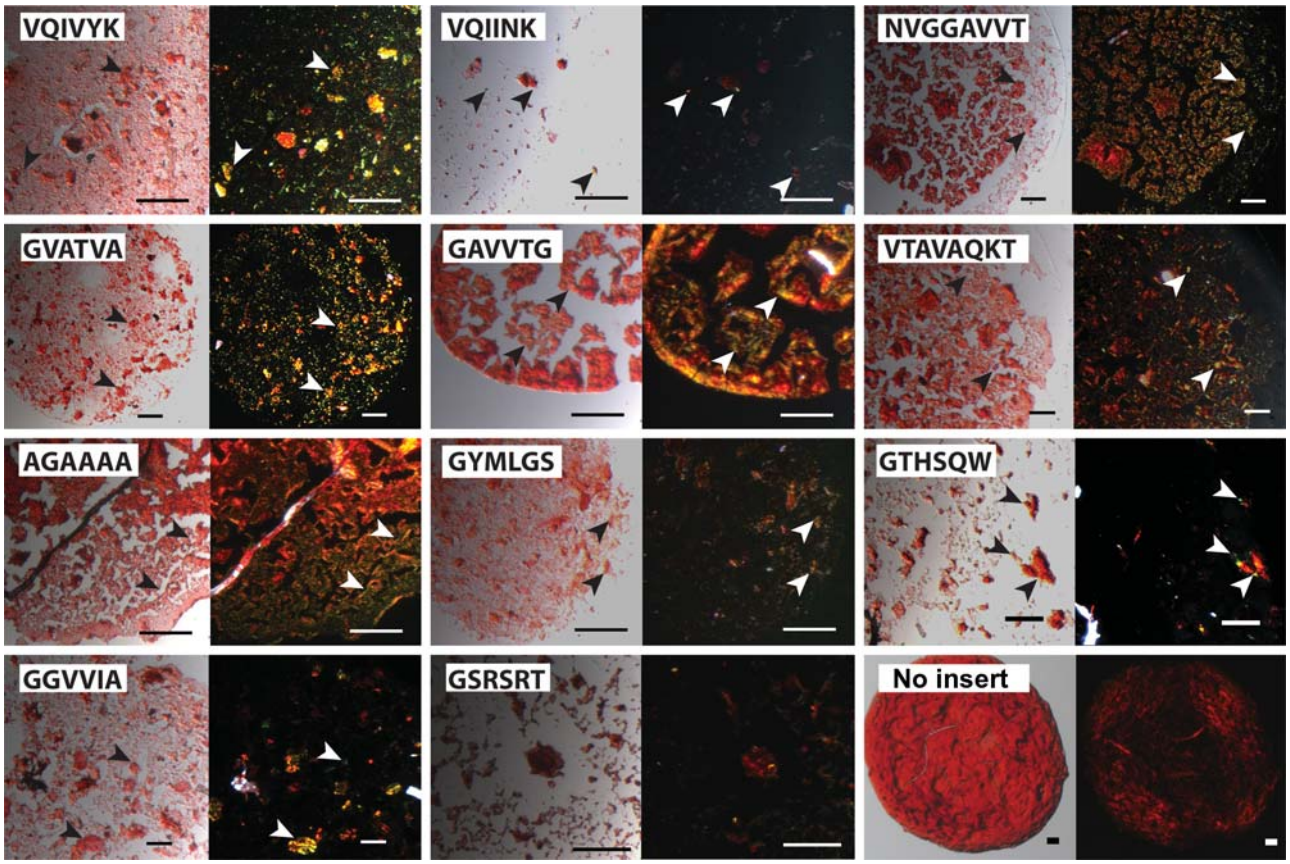

Fig. 3. RNase A fibrils display Congo red birefringence, characteristic of amyloid fibrils. Congo red binds to each RNase A aggregate, shown in the bright field panels. Every sample exhibits a yellow to apple-green birefringence when placed between crossed polarizers. Arrowheads point to areas of dye and corresponding birefringence. Variance in birefringent intensities may be related to the abundance of sample present. All scale bars are 100 μm.

interactions. Weak Congo red birefringence suggests more order in the GSRSRT aggregates observed. The new interactions, however, are insufficient for fibril formation.

Summary

We have identified fibril-forcing segments in the fibrillizing proteins tau, α-syn, PrP and Aβ. These segments form fibrils when in isolation from the rest of the protein (Sawaya *et al*., 2007) and when inserted in the C-terminal hinge loop of wild-type RNase A. From these observations, we postulate that under the right conditions, many proteins expose fibril-forcing segments, which may be sufficient to cause aggregation and fibril formation, as observed for normally soluble proteins by Astbury and Dickinson (1935), Dobson (1999) and Wang *et al.* (2008), as well as others.

Acknowledgements

We thank Magdalena Ivanova, Stuart Sievers, Marcin Apostol, Mari Gingery, Shilpa Sambashivan and Lukasz Goldschmidt for discussion and technical help.

Funding

This work was supported by the National Science Foundation (MCB-0445429); the National Institute on Aging (1R01 AG029430) and the United States Department of Energy Office of Biological and Environmental Research.

References

Astbury,W.T. and Dickinson,S. (1935) *Biochem. J.*, **29**, 2351–2360.
Balbirnie,M., Grothe,R. and Eisenberg,D.S. (2001) *Proc. Natl Acad. Sci. USA*, **98**, 2375–2380.
Conway,K.A., Harper,J.D. and Lansbury,P.T. (1998) *Nat. Med.*, **4**, 1318–1320.
Crestfield,A.M., Stein,W.H. and Moore,S. (1962) *Arch. Biochem. Biophys.*, (Suppl. 1), 217–222.
Dobson,C.M. (1999) *Trends Biochem. Sci.*, **24**, 329–332.
El-Agnaf,O.M., Jakes,R., Curran,M.D. and Wallace,A. (1998) *FEBS Lett.*, **440**, 67–70.
Glenner,G.G., Eanes,E.D. and Page,D.L. (1972) *J. Histochem. Cytochem.*, **20**, 821–826.
Ivanova,M.I., Thompson,M.J. and Eisenberg,D. (2006) *Proc. Natl Acad. Sci. USA*, **103**, 4079–4082.
Kanski,J., Aksenova,M. and Butterfield,D.A. (2002) *Neurotox Res.*, **4**, 219–223.
Kim,H.Y., Heise,H., Fernandez,C.O., Baldus,M. and Zweckstetter,M. (2007) *Chembiochem*, **8**, 1671–1674.
Klunk,W.E., Pettegrew,J.W. and Abraham,D.J. (1989) *J. Histochem. Cytochem.*, **37**, 1273–1281.
Lansbury,P.T. Jr, Costa,P.R., Griffiths,J.M., Simon,E.J., Auger,M., Halverson,K.J., Kocisko,D.A., Hendsch,Z.S., Ashburn,T.T. and Spencer,R.G., *et al*. (1995) *Nat. Struct. Biol.*, **2**, 990–998.
Li,J., Uversky,V.N. and Fink,A.L. (2001) *Biochemistry*, **40**, 11604–11613.
Libonati,M. and Gotte,G. (2004) *Biochem. J.*, **380**, 311–327.
Liu,Y., Hart,P.J., Schlunegger,M.P. and Eisenberg,D. (1998) *Proc. Natl Acad. Sci. USA*, **95**, 3437–3442.
Liu,Y., Gotte,G., Libonati,M. and Eisenberg,D. (2001) *Nat. Struct. Biol.*, **8**, 211–214.
Luhrs,T., Ritter,C., Adrian,M., Riek-Loher,D., Bohrmann,B., Dobeli,H., Schubert,D. and Riek,R. (2005) *Proc. Natl Acad. Sci. USA*, **102**, 17342–17347.
Marshall,G.R., Feng,J.A. and Kuster,D.J. (2008) *Biopolymers*, **90**, 259–277.
Narhi,L. *et al.* (1999) *J. Biol. Chem.*, **274**, 9843–9846.

Nelson,R., Sawaya,M.R., Balbirnie,M., Madsen,A.O., Riekel,C., Grothe,R. and Eisenberg,D. (2005) *Nature*, **435**, 773–778.
Rohl,C.A., Strauss,C.E., Misura,K.M. and Baker,D. (2004) *Methods Enzymol.*, **383**, 66–93.
Sambashivan,S., Liu,Y., Sawaya,M.R., Gingery,M. and Eisenberg,D. (2005) *Nature*, **437**, 266–269.
Sandal,M., Valle,F., Tessari,I., Mammi,S., Bergantino,E., Musiani,F., Brucale,M., Bubacco,L. and Samori,B. (2008) *PLoS Biol.*, **6**, e6.
Sawaya,M.R., *et al*. (2007) *Nature*, **447**, 453–457.
Sekijima,Y., Wiseman,R.L., Matteson,J., Hammarstrom,P., Miller,S.R., Sawkar,A.R., Balch,W.E. and Kelly,J.W. (2005) *Cell*, **121**, 73–85.
Serpell,L.C., Berriman,J., Jakes,R., Goedert,M. and Crowther,R.A. (2000) *Proc. Natl Acad. Sci. USA*, **97**, 4897–4902.
Si,K., Lindquist,S. and Kandel,E.R. (2003) *Cell*, **115**, 879–891.
Smith,B.D. and Raines,R.T. (2006) *J. Mol. Biol.*, **362**, 459–478.
Sunde,M., Serpell,L.C., Bartlam,M., Fraser,P.E., Pepys,M.B. and Blake,C.C. (1997) *J. Mol. Biol.*, **273**, 729–739.
Thompson,M.J., Sievers,S.A., Karanicolas,J., Ivanova,M.I., Baker,D. and Eisenberg,D. (2006) *Proc. Natl Acad. Sci. USA*, **103**, 4074–4078.
Vilar,M., Chou,H.T., Luhrs,T., Maji,S.K., Riek-Loher,D., Verel,R., Manning,G., Stahlberg,H. and Riek,R. (2008) *Proc. Natl Acad. Sci. USA*, **105**, 8637–8642.
von Bergen,M., Friedhoff,P., Biernat,J., Heberle,J., Mandelkow,E.M. and Mandelkow,E. (2000) *Proc. Natl Acad. Sci. USA*, **97**, 5129–5134.
von Bergen,M., Barghorn,S., Li,L., Marx,A., Biernat,J., Mandelkow,E.M. and Mandelkow,E. (2001) *J. Biol. Chem.*, **276**, 48165–48174.
Wang,L., Maji,S.K., Sawaya,M.R., Eisenberg,D. and Riek,R. (2008) *PLoS Biol.*, **6**, e195.
Westermark,P., Benson,M.D., Buxbaum,J.N., Cohen,A.S., Frangione,B., Ikeda,S., Masters,C.L., Merlini,G., Saraiva,M.J. and Sipe,J.D. (2007) *Amyloid*, **14**, 179–183.

Received June 11, 2009; revised June 11, 2009; accepted June 12, 2009

Edited by Valerie Daggett